X-1393

UNCLASSIFIED

MonP-172

Subject Category: PHYSICS

UNITED STATES ATOMIC ENERGY COMMISSION

YIELD OF PHOTONEUTRONS FROM U^{235} FISSION PRODUCTS IN HEAVY WATER

By
S. Bernstein
W. M. Preston
G. Wolfe
R. E. Slattery
E. Greuling

September 24, 1946

Clinton Laboratories
Oak Ridge, Tennessee

Technical Information Service, Oak Ridge, Tennessee

UNCLASSIFIED

Date Declassified: January 12, 1956.

Printed in USA, Price 30 cents. Available from the Office of Technical Services, Department of Commerce, Washington 25, D. C.

MonP-172

Contract No. W 7405 - Eng. 39

Section IV

L. B. Borst, Section Chief

FINAL REPORT

YIELD OF PHOTONEUTRONS FROM U^{235} FISSION PRODUCTS IN HEAVY WATER

S. Bernstein, W. M. Preston, G. Wolfe, R. E. Slattery

with Appendix

NEUTRON YIELD FROM MULTIPLY SCATTERED COMPTON PHOTONS

E. Greuling

PROBLEM ASSIGNMENT PX10-15

September 24, 1946

CLINTON LABORATORIES
Oak Ridge, Tennessee

TABLE OF CONTENTS

Yield of Photoneutrons from U^{235} Fission Products in Heavy Water

S. Bernstein, W. M. Preston, G. Wolfe, R. E. Slattery.

ABSTRACT

The half-lives and yields of the photoneutrons created in heavy water by U^{235} fission product gamma rays have been measured. Seven half-lives have been found: 2.5 sec., 41.2 sec., 2.38 min., 7.7 min., 27.3 min., 1.65 hr., 4.37 hr., and 53 hr. The shortest one and longest one of these are least reliable. Eighty-five percent of the photoneutrons appear in the two shortest half-lives, the 2.5 sec. component being three times as intense as the 41 sec. component. The total saturated activity of the photoneutrons for an infinite amount of heavy water was calculated from measurements with a 10" radius sphere to be about 16.5% of the saturated delayed neutron activity. The data indicate that there must be of the order of two gamma rays, of energy above 2.17 Mev, emitted per fission by fission products with half-lives longer than one sec.

Yield of Photoneutrons from U^{235} Fission Products in Heavy Water

S. Bernstein, W. M. Preston, G. Wolfe,
R. E. Slattery.

I. Introduction

In a pile consisting of uranium and heavy water, gamma rays of energy greater than 2.17 Mev given off by the fission products will create neutrons in the heavy water by photo-disintegration of the deuteron. These photoneutrons will have the same periods as the gamma rays which create them. They will, therefore, act in all respects like the delayed neutrons themselves, and may exert an appreciable effect on the kinetic behavior of the pile. In order to estimate the effect of the photoneutrons upon pile periods, their number as a function of time must be known, as in the case of the delayed neutrons. The purpose of this experiment was to measure the number of photoneutrons created in heavy water by U^{235} fission products as a function of the length of time after bombardment. Since the photoneutrons are, for short times after bombardment, accompanied by delayed neutrons, the yields were measured relative to those of the delayed neutrons. For this purpose, the yields of delayed neutrons as given by Hughes, Dabbs and Cahn in CP-3094 were used. The results of CP-3094 have been collected in Table I for convenience.

II. Apparatus

A schematic diagram of the apparatus is shown in Fig. 1. It consisted of a ten inch radius, 1/8 inch wall, aluminum sphere immersed in a large tank of oil. A "rabbit" containing a sample of enriched uranium oxide could be transferred from the center of the pile to the center of the sphere in about 0.25 sec. by means of a pneumatic tube. The sphere could be filled or emptied of heavy water in about one minute by means of a siphon arrangement.

The neutron distribution in the oil was studied by means of fission chambers, each containing about 64 mg of 90% enriched uranium. Fission chambers were chosen in preference to BF_3 counters because of their greater insensitivity to the large gamma ray "background" being emitted by the sample. The ion chamber could be placed at chosen reproducible radial positions in the tank by means of a track and carriage arrangement.

Since some of the periods involved are fractions of a sec., it was necessary to keep the initial counting rates quite high in order to obtain good statistics throughout the run. To keep corrections for missed counts low, the fastest most readily available amplifier was used. A modified Simpson proportional counter amplifier and scaling circuit were adapted and found to have a resolving time of about 20 microseconds. This resolving time was determined by exposing a sample of uranium first at high pile power, then at low power, and plotting the ratio of the activities as a function of time as described in CP-3094. All of the data were then corrected for missed counts using this over-all experimentally determined "resolving time".

Fission pulses from the amplifier were fed into a scale of 256 The data was recorded by photographing the scaling-circuit interpolation bulbs with an open shutter oscilloscope camera. The film moved past the neon bulbs in such a manner that each bulb appeared as a dashed line on the film for the period the bulb was lit. A time signal was also impressed on the film every 0.1 sec by means of a neon bulb and a revolving shutter driven by a synchronous motor. The length of the exposure was recorded automatically on the film by another neon bulb which lighted at the start and went out at the end, by connections with the electropneumatic control switches. A reproduction of one of the films is shown on Fig. 2.

III. Method

The method employed to measure the source activity is based on the following theory. Consider a point source of Q neutrons/sec, having an arbitrary energy distribution (above thermal energy), surrounded by an oil bath large enough to absorb all the neutrons. It is known that most of the absorption is due to hydrogen nuclei in the oil, and that the H-capture cross section is very small above thermal energy. Then the rate of production of fast neutrons must equal the rate at which they are captured, or $Q = \int (nv)_t \, \sigma_c \, dV$, where $(nv)_t$ is the flux of thermal neutrons at any point in the oil, σ_c is the macroscopic cross section for capture at thermal energy, and the integral is extended over the oil volume. Measurements with a fission chamber detector give a counting rate "Y" at any point in the oil which is proportional to $(nv)_t$, provided

correction is made for the epicadmium counting rate. In the case of spherical symmetry, $q \propto \int Y R^{-2} dR$ In our case, since there is negligible neutron absorption in the heavy water sphere, the integral is taken from R_0 to ∞, where R_0 is the sphere radius.

The ion chamber was fixed in a given radial position, an exposure was made, and the resulting neutron counting rate recorded on the moving film as a function of time "t" after the end of the exposure. When the activity had decreased to an acceptable value, the ion chamber was moved to the next radial position and another exposure made with the same sample. A single series usually comprised exposures in four to eight positions. A complete experiment required three complete series: (a) with heavy water in the sphere, in which case both delayed and photoneutrons are present; (b) with the sphere empty, so that the activity is that due to delayed neutrons alone (c) with the sphere empty and the fission chamber surrounded by cadmium, in order to measure the delayed neutrons with epicadmium energies. With heavy water in the sphere the number of epicadmium neutrons was negligible.

The constancy of the pile power level and the detecting instruments was checked by repeating the initial exposure at the end of each experiment. Instrument sensitivity alone was checked by means of a Ra-α-Be source. Variations remained within one percent, which simplified the experiment by making it unnecessary to use an exposure monitor.

For each exposure, a plot was made from the film data of the counting rate at the particular radial position as a function of "t". From the group of curves forming a series, other curves were constructed of (counting rate x R^2) vs R, for successive fixed values of "t". Here, R is the radial distance of the detector from the source at the center of the sphere. The source activity at any time is then proportional to the area under the corresponding curve.

Examples of these (counting rate x R^2) vs R curves are shown in Fig. 3. With heavy water in the sphere, the curves on a semi-log scale are linear with a relaxation length (inverse slope) which is constant and equal to approximately 1.25 inches. This indicates that the neutrons have been well thermalized before they escape into the surrounding oil. When the sphere is empty, the semi-log plot of the neutron distribution shows a decided initial curvature due to slowing down in the oil.

In general, the desired source activity due to photoneutrons alone, at a time "t_1", is the difference between the areas under the corresponding distribution curves, with and without heavy water, after correction for epicadmium activity. By computing a number of points, a curve may be drawn of source photoneutron activity as a function of time. We assume that the data can be represented by a formula of the form (1), where A_p is the photoneutron activity of the source as a function of time "t" after the end of the exposure.

$$A_p(t) = \sum_i a_i(1 - e^{-T/\tau_i})e^{-t/\tau_i} \qquad (1)$$

T the exposure time, τ_i the mean life, and a_i the yield of the i'th radioactive period for infinite exposure time. If the experimental curve is linear on a semi-log plot at sufficiently large values of "t", the longest half-life period can be determined. The half-lives of shorter periods are evaluated by the well-known "peeling off" process. A similar formula for $A_d(t)$, the delayed neutron activity, can be fitted to the volume integral curve from the data taken with the sphere empty. By evaluation at $t = o$, $T = \infty$, we can then express the yields a_i of each photoneutron period as fractions of the total calculated delayed neutron yield $A_d(t = o, T = \infty)$.

At small values of "t" the photoneutron activity of the source is as little as one-tenth of the delayed neutron activity. That is, the difference of the areas under two curves of the type shown in Fig. 3, with and without heavy water, is only 10% of either area. Thus an error of 1 percent in either area causes a 10% error in the result, and it is desirable to obtain the maximum number of experimental points in order to increase accuracy. At larger values of "t", however, the delayed neutron activity becomes a small and finally vanishing fraction of that due to the photoneutrons, which contain several components of comparatively long mean life. In this case, a sufficiently accurate value of the volume integral of the counting rate with heavy water can be obtained from the counting rate at a single radial position, as is clear from Fig. 3. Since the slope is approximately constant and known, a single point determines the area under a curve, where "t" must be extended to many

hours, this procedure results in a considerable saving of time.

IV. Experimental Results

(A) Periods and Uncorrected Yields

Fig. 4 is a plot of the photoneutron activity, measured at a single radial position with D_2O in the sphere, as a function of time. The sample was 2.7 gm of roughly 60% 25 exposed in the pile for 3.75 hours. Within the interval 4 hours to 26 hours, the gross activity, Curve #1, is well represented by three periods of half-life 53 hr., 4.37 hr., and 1.66 hr. The longest period may be considerably in error because it was followed over a range of only 2 in activity, and the activity at the end was only a few times background. The other two periods were followed over a factor of 100, and should be accurate. The relative yields were computed by extrapolation of the individual terms to zero time and infinite exposure.

Fig. 5 illustrates a 30 min exposure of a 0.7 gm sample, also measured at a fixed radial position. Curve #1 is the gross activity. A formula representing the three previously determined photoneutron periods was fitted to Curve #1 at t = 6.5 hr. by the adjustment of a constant multiplier, which allows for the different sample size and pile power level. Curve #2 is the result of subtracting from #1 these three longer periods. It indicates a fourth period of 27.3 minutes half-life, with signs of a still shorter period at $t < 1$ hr.

Fig. 6 illustrates a 5 min exposure of a .7 gm sample. Curve #1 is the crude data. Curve #2 is the result of subtracting off the four

previously determined periods by means of a formula adjusted to fit at t = 129 min. A fifth period of half-life 7.7 min is demonstrated.

Thus far we have determined the yields of 5 photoneutron periods relative to each other. In the next experiment, the yields are related to that of the delayed neutrons. Fig. 7 shows results of a 3 min exposure with a 0.7 gm sample, from t = 3 min to 1 hour. In the first part of this interval the delayed neutron activity is not negligible. It was measured in the following manner. A series of 7 exposures was made, without D_2O in the sphere, varying the radial distance R of the detector from the source and measuring with a mechanical recorder the number of counts in the interval t = 2.5 to t = 4.0 min. This time integral of the delayed neutrons was plotted as a (counting rate x R^2) vs R curve, the area N under the curve being proportional to the time and volume integral of the delayed neutron activity of the source. A six term formula similar to Eq. (1) was set up for $A_d(t)$, using the constants for the delayed neutron periods as given in Table I, and integrated from t = 2.5 to 4.0 min. Letting $N = C_1 \int A_d(t)dt$, the constant C_1 was determined for this experiment. $C_1 A_d(t)$ then represents the volume integrated delayed neutron activity as a function of time.

Curve #1 of Fig. 7 shows the gross source activity with D_2O in the sphere. This was actually computed from the counting rate measured at a single radial position, an approximation previously discussed. If we subtract from this the delayed neutron activity $C_1 A_d(t)$, computed as above, the result is Curve #2, representing photoneutrons alone. Curve #3 is the result of subtracting off the 5 previously determined photoneutron periods, fitting the formula at t = 53 min. A sixth period is indicated of half-life 2.38 min.

Since we have a formula representing the volume integrated activity of the delayed neutrons and one for 6 photoneutron periods, we can now extrapolate to t = o and infinite exposure time and determine the photoneutron yields relative to the delayed neutrons. Table II lists these six periods with their yields A relative to the yield of the 22 sec delayed neutron period as 1.00.

In the next experiment, no short cuts were permissible because of the need for accuracy. Fig. 8, Curve #1, shows the gross integrated activity, with D_2O in the sphere, resulting from a 30 sec exposure of a 0.15 gm enriched sample. Each point on the curve represents an integral of (counting rate) x R^2 vs R, taken from curves of the type shown in Fig. 3. Curve #2 shows, for the same exposure, the volume integrated activity without D_2O, due to delayed neutrons alone. Curve #2 has been corrected for epi-cadmium activity, which amounted to about 2%. Curve #3, Fig. 8, shows the total photoneutron activity, Curve #1 minus #2. It is seen that the difference is only 10% of the total activity at t = 30 sec.

The delayed neutron formula was fitted to the experimental Curve #2, and the saturated delayed neutron activity computed for this experiment. From previous results, a formula expressing the photoneutron activity could be set up for the 2.4 min and longer periods. Subtracting these off from Curve #3, the result was Curve #4, which represents a new period of half-life 41 sec and yield A = 0.090 (see Table II). There is evidence for a still shorter period below t = 30 sec., but in this experiment the counting rate became so high in this region that the data are not reliable.

A series of 30 sec exposures was made with a 1.5 gm sample of unenriched uranium. Curve #1, Fig. 9, is the total integrated activity with D_2O. Curve #2, that without. Curve #3 their difference. The delayed neutron formula, using the values in Table I, was fitted to Curve #2 at t = 10 sec. It is of interest as a check on Table I that the formula then agreed with the experimental results to 1% or better from t = .5 sec to t = 12 sec and with the time integrated activity from t = 30 to t = 50 sec.

A formula for the photoneutron activity due to the 7 previously determined periods was obtained by fitting it to the observed time integrated activity in the interval t = 30 to t = 50 sec. This was subtracted from Curve #3, Fig. 9, to yield the new period, Curve #4, of half-life 2.5 sec and A = 0.225 (See Table II).

(B) Estimated Accuracy

The accuracy to be expected in obtaining one of the areas under curves of the type in Fig. 3 is about one percent, due to statistical probable errors alone. Since the short period photoneutron yields were obtained as the difference of two areas, amounting to about 10 percent of either, these yields are uncertain by at least 10 percent. The yields of the longer periods, except for the 53 hr period, should be somewhat more accurate.

If the heavy water was 99.87 percent pure, as stated by the manufacturer, the absorption of neutrons in it would have been negligible.

Since contamination might have been introduced during the course of the experiment, the neutron absorption of the heavy water was tested in the following manner: An Sb-Be photoneutron source was placed at the center of the sphere and the neutron distribution curves in the oil were obtained, with and without heavy water. Since the γ-rays from Sb are less than 2.17 mev, they cannot create any photoneutrons in the heavy water, and the areas under the (counting rate) $\times R^2$ vs R curves should be equal in the two cases. Actually the areas were found to be the same within about 2 percent.

(C) Corrections to Experimental Yields

In Table II, Column A represents photoneutron yields (saturated activities) for our sphere of heavy water relative to the 22 sec delayed neutron period yield as 1.00. In order to correct these yields to the case of an infinitely large sphere of D_2O and complete γ-ray absorption, it is necessary to know the energy of the γ-rays. Conclusions about the initial energy of the photoneutrons could not be made from the data of this experiment. The large amount of heavy water moderator slowed the neutrons down to such an extent that the shape of the distribution curve in the oil where the measurements were taken was no longer a measure of the initial neutron energy. Hence, we have tried to correlate our periods with those reported by Hughes, Spaatz and Cahn in CP-3472, April 25, 1946. Table III shows this correlation. Although the agreement in the half-lives is only fair, it is sufficient to set up a correspondence between

our periods and theirs. Accordingly, we have used their values for the γ-ray energies. In the case of the two longest periods, as shown in Table II, we have assumed entirely arbitrarily an energy E_γ = 3 mev for purposes of computation.

In D_2O and for γ-ray energies between 2 and 5 mev the photoelectric effect and pair production are negligible in comparison with the Compton effect. If we assume that every Compton scattering of a γ-ray quantum by an electron reduces the quantum energy below the γ,n threshold in D_2O, the fraction of the quanta absorbed in a sphere of radius R cm, from a central point source, is $F_t = 1 - e^{-(\mu_s + \mu_\gamma)R}$ where μ_s is the linear "absorption" coefficient/cm for Compton scattering and μ_γ is the coefficient for the γ,n reaction in D_2O. For this experiment the effective thickness of heavy water is 23.3 cm. $\mu_s = \sigma_s \times 3.35 \times 10^{23}/cm^3$ for D_2O, where σ_s, the Compton scattering cross section/electron varies from 1.27×10^{-25} cm^2 at 2.5 mev to 1.06×10^{-25} at 3.5 mev. $\mu_\gamma = 6.7 \times 10^{22} \times \sigma_\gamma/cm^3$, where σ_γ, the γ,n cross section/deuteron varies from zero at 2.17 mev to about 14×10^{-28} cm^2 at 3.5 mev. In Table II are listed values of $1/F_t$ the correction factor by which the yields A must be multiplied to give the yields for an infinite sphere of D_2O, for the assumed energies E_γ.

A small correction, $\alpha = 1.06$, is listed in the next column of Table II. This compensates for the γ-ray absorption in the 0.050 inch wall thickness of the pneumatic tube, the fixed 0.125 inch thick Al tube

through the center of the sphere, and in the 3/16 inch thick wall of the bakelite rabbit.

Column β in Table II gives an additional correction necessary because not every Compton scattering process reduces the energy of a γ-ray quantum below the γ,n threshold, so that the flux of γ-rays of energy above the threshold is everywhere higher than we would calculate using the full Compton scattering cross section. β/F_t is then the ratio of the number of γ,n neutrons produced in an infinite D_2O sphere to that produced in a sphere of radius 23.3 cm. taking into account multiple scattering. The theory of this correction, developed by Soodak and Greuling, is given in Appendix A.

Column Ac in Table II is A x $\alpha\beta/F_t$, the corrected yield of photoneutrons in an infinite sphere of D_2O. Column A_d is 100 Ac/4.54, the percent yield relative to the total number of delayed neutrons (See Table I, total of Col. A). Column A_f is 2.43 x 0.00755 A /100, the absolute yield of photoneutrons per fission, taking ν (25) = 2.43 and the delayed neutron yield from Table I.

(D) Gamma Ray Yields

We now compute the number of γ-rays per fission necessary to produce the photoneutrons of each period, with yields A_f in Table II. The fraction of the total γ-ray quanta from a point source which are absorbed in the γ,n reaction in an infinite D_2O sphere is

$$F_\gamma = \int_0^\infty e^{-(\mu_s + \mu_\gamma)R} \mu_\gamma \, dR = \frac{\mu_\gamma}{\mu_\gamma + \mu_s}$$

provided each scattering process is assumed to reduce the energy below the threshold. If we take into account the fact that some scattered quanta still have energy above the threshold, the actual photoneutron production will be higher by a factor E, which will be small near the threshold and increase with the initial energy of the γ-ray. In Table II are listed, for each period, the values of $1/F_\gamma$ and of E. The absolute yield of γ-ray quanta per fission, A_γ, will be

$$A_\gamma = A_f/F_\gamma E \ .$$

V Discussion of Results

(A) Summary

A summary of the results obtained is given in Table II. An explanation of the meaning of each column is given with the table. The results may be summarized as follows:

(1) The photoneutron periods observed show half-lives from 2.5 sec to 53 hrs.

(2) Eighty-five percent of the photoneutrons appear in the shortest half-lives of 2.5 sec and 30 sec, the 2.5 sec half-life component being three times as intense as the 30 sec half-life.

(3) The total saturated activity of the photoneutrons for an infinite amount of heavy water is about 16% of the saturated delayed neutron activity.

(B) The Effect of Possible Parent-Daughter Contributions

It should be pointed out that in the analysis of the data as described above it has been assumed that the hard gamma ray emitters are initial fission fragments. The interpretation of the data is made somewhat uncertain because of the possibility that the hard photon giving the photoneutron may come from a daughter of the initial fragment. In such cases the data may yield the true period, but the amplitude deduced by extrapolating the decay curve back to zero time will be in error. If the daughter has a very much longer life than its parent, the error will not be large. If the two have comparable lifetimes the saturated activities given may be a considerable overestimate. If both the parent and daughter give hard gamma rays, both amplitudes will be in error, but the sum of the two exponential terms will give a correct description of the activity as a function of time.

(C) Number of Photons Per Fission

From the number of photoneutrons per fission, the number of photons per fission was calculated from considerations of the relative probabilities of Compton and γ,n collisions. The results for each period are given in the column A_γ of Table II. The sum of the values in this column is 2.3 photons per fission. For the sixth period listed, Hughes, Spaatz and Cahn give two values for the γ-ray energy, one from photoneutron energy measurements (2.25 mev) and one from direct γ-ray absorption measurements (2.4 mev). The γ,n cross section is changing very rapidly in this region, so that the calculated number of photons per fission is very sensitive to

which of these two values is used. Even if the value giving the lesser number of photons per fission is used, the total number of photons per fission adds up to 1.7. As a total, this number may not be unreasonable. However, the 0.62 photons per fission given for the single 2.5 sec period is much too high to be due to a single isotope. The same conclusion could be made also for the 41 sec and the 2.4 min periods, since the highest fission yields observed are about six percent. These considerations suggest that there may be many fission products having periods of several seconds to several minutes, with γ-rays above 2.2 mev. If close together, such periods could not be resolved in this experiment.

If the suggestion that 25 may have many short period γ-rays is true, and since these short periods have been shown to account for 90% of the photoneutrons, then the results of this report might be used to speculate about photoneutron yield of 23, for which there are no observations available at the present time, by the following considerations: The 2.5 sec and 41 sec periods, which account for 90% of the photoneutrons, give about 1 photon per fission. Since maximum fission product yields are about 6%, there are about 17 fission chains contributing the hard γ-rays in the case of 25 if we assume one photon per fission chain. The effect of one of these is, then, at most 5 to 10% and the shift in the maximum of the fission product yield curve of a few mass number units, in going from 25 to 23, is not likely to have any considerable effect. The number of photoneutrons from 23 might, therefore, be expected to be roughly the same as for 25. The number of delayed neutrons

for 23 has been reported to be about one-third that for 25 (CP-3147). Consequently, it seems that for 23 the number of photoneutrons may be comparable to the number of delayed neutrons.

(D) Comparison with CP-3472

This work was done simultaneously with that of Hughes, Spaats and Cahn at the Argonne Laboratory (CP-3472). Our results are compared with theirs in Table III. The agreement between the periods is fair, considering the large number of delayed and photoneutron periods involved. The main disagreement in the periods is that our data showed a 4.4 hr period not reported by them. It seems very probable that really accurate determination of the periods, especially the shorter ones, would necessitate chemical separation of individual fission products, or groups of products. The greatest disagreement on yield values lies in the region where the measurements are made difficult because the photoneutrons represent only a small part of all the neutrons present. The 30 sec period of CP-3472 is three times as intense as our 41 sec period. The sum of the values listed in Column A of Table II gives the result that the total saturated photoneutron activity is 16% of the saturated delayed neutron activity. CP-3472 gives 28% for this ratio.

TABLE I

Delayed Neutrons from 25

τ	$\tau_{\frac{1}{2}}$	E	A	B
80.2	55.6	.25	0.153	2.5×10^{-4}
31.8	22.0	.56	1.00	16.6
6.50	4.51	.43	1.28	21.3
2.19	1.52	.62	1.45	24.1
0.62	0.43	.42	0.51	8.5
0.072	0.06		0.16	2.5
Totals			4.54	75.5×10^{-4}

τ = period, $\tau_{\frac{1}{2}}$ = half life, E = energy in mev.

A = saturated yield relative to the yield of the 22 sec period as 1.00

B = absolute yield relative to the total number of neutrons emitted per fission

Data from CP-3094 (Hughes, Dabbs & Cahn 7-30-45) and CF-3405 (Hall, Dec. 1945).

Table II

Photoneutron Yields and Periods

Ref. No.	$T_{\frac{1}{2}}$	T	A	E_γ	$1/F_t$	α	β	A_c	% A_d	x 10^4 A_f	$1/F_\gamma$	E	A_γ
1	53h	76h	.00038	(3)	1.695	1.06	1.085	00074	.0163	.0298	476	1.14	.00125
2	4.37h	6.3h	.00119	(3)	1.695	1.06	1.085	.00232	.0515	.0942	476	1.14	.00394
3	1.65h	2.4h	.0093	2.62	1.62	1.06	1.052	.0168	.370	.676	670	1.09	.0415
4	27.3m	39.3m	.0082	2.66	1.63	1.06	1.056	.0149	.328	.600	643	1.09	.0354
5	7.7m	11.1m	.0124	3.0	1.695	1.06	1.085	.0242	.534	.975	476	1.14	.0407
6	2.4m	3.44m	.0276	2.65	1.63	1.06	1.054	.0504	1.11	2.03	650	1.09	.121
7	41 s	59.5s	.090	2.25	1.52	1.06	1.009	.147	3.24	5.93	2450	1.015	1.43
8	2.5 s	3.6 s	.225	3.4	1.77	1.06	1.11	.469	10.31	18.9	389	1.18	.623
							Total		15.96%	29.2×10^{-4}			2.3

$T_{\frac{1}{2}}$ = half life. T = mean life

A = uncorrected photoneutron yield, relative to a yield of 1.00 for the delayed neutron 22 sec period

E_γ = γ-ray energies, in mev. from CP-3472. Values in parentheses are arbitrary

α = Correction for γ-ray absorption in the rabbit wall and in the Al tubes at the center of the sphere

β = Correction for multiple scattering (see Appendix A)

A_c = $A \times \alpha \times \beta / F_t$, the corrected yield in an infinite D_2O sphere

A_d = $100\ A_c/4.54$ = percent yield of photoneutrons relative to total delayed neutrons

A_f = $2.43 \times .00755 \times A_d/100$ = absolute photoneutron yield per fission

$\frac{1}{F_\gamma}$ = Number of photons per photoneutron in ∞ D_2O on the basis that single Compton collision knocks γ-energy below threshold

E = Correction factor to account for γ's not knocked below threshold on single collision

A_γ = Absolute number of photons per fission

TABLE III

Comparison of Results, This Paper & CP-3472

	This Paper			Hughes, Spaatz & Cahn			
Ref. No.	$T_{\frac{1}{2}}$	A_c		$T_{\frac{1}{2}}$	A_c	E_γ	
1	53 h	.00074		24 h	.00032	-	
2	4.37 h	.00232		-		-	
3	1.65 h	.0168		2.0 h	.0091	2.62	
4	27.3 m	.0149		32 m	.0118	2.66	
5	7.7 m	.0242		6.5 m	.0210	3.0	
6	2.4 m	.0504		90 s	.0720	2.65	
7	41 s	.147		30 s	.456	2.25	
8	2.5 s	.469		6.7 s	.655	3.4	

$T_{\frac{1}{2}}$ = half-life

A_c = corrected yield, infinite D_2O absorber, relative to the yield of the 22 sec delayed neutron period as 1.00

E_γ = γ-ray energy in mev

APPENDIX A

Neutron Yield from Multiply Scattered Compton Photons

E. Greuling

The neutron yield resulting from the photodisintegration of deuterium in a sphere of heavy water can be calculated by making use of the following simple assumptions:

(a) Every Compton scattered photon of incident energy greater than 2 mev suffers negligible change in direction. Actually 4 mev photons are scattered by less than 30^0 if their resulting energy is above the γ,n threshold, 2.2 mev.

(b) The differential cross-section for scattering of photons of energy E' into the energy range E to E + dE is independent of the lower energy E, and is equal to

$$\sigma(E' \rightarrow E)dE \approx \frac{2\pi r_o^2}{E'^2}\, dE, \quad 4.3 \leq E' \leq 7 \qquad (1)$$

Here $r_o = e^2/mc^2$, and E' and E are the incident and scattered photon energy in mc^2 units. The maximum deviation of the correct Klein-Nishina formula from equation (1) is 3.5% which occurs for E' = 7 and E = 4.3.

(c) The total Compton cross-section, as a function of γ-ray energy, E between 4.3 and 7 mc^2, differs by less than 2% from the approximate formula,

$$\sigma(E) = 2\pi r_o^2 \left[1/(\alpha E) + 0.089\right] \qquad (2)$$

where $\alpha = 5/4$.

Consider a point source of γ-rays of energy E_o at the center of a sphere of D_2O. The number of photons per unit source strength crossing a spherical surface at r that have suffered no collisions is $e^{-\mu_o r}$ where μ_o is the reciprocal mean free path of photons of energy E_o. According to Equ. (2)

$$\mu = 2\pi r_o^2 N \left[1/(\alpha E) + 0.089\right] + \mu_\gamma(E) \qquad (3)$$

where N is the number of electrons per cm^3, and $\mu_\gamma(E)$ is the γ,n inverse absorption mean free path for photons of energy E. Hereafter $\mu_\gamma(E)$ is dropped from Equ. (3) because it at most amounts to only a 0.3% correction on μ.

Let $F(r,E)dE$ be the number of photons of energy E to E + dE that cross the spherical surface at r after having suffered at least one collision. The balance between scattered photons entering and leaving the cell of extension dEdr is, upon inserting Equ. (1), given by:

$$\frac{\partial F}{\partial r} + \mu(E)F = \frac{2\pi r_o^2 N}{E_o} \int_E^{E_o} \frac{E_o dE'}{E'^2} P(r,E') + \frac{2\pi r_o^2 N}{E_o^2} e^{-\mu_o r} \qquad (4)$$

If one defines a new variable,

$$z = \mu - \mu_o \approx \frac{2\pi r_o^2 N}{\alpha} (1/E - 1/E_o), \qquad (5)$$

and substitutes into equation (4) the form,

$$F = \frac{2\pi r_o^2 N}{E_o^2} e^{-\mu_o r} \varphi(r,z), \qquad (6)$$

one obtains the following integro-differential equation for φ :

$$\frac{\partial \varphi}{\partial r} + z\,\varphi = 1 + \alpha \int_0^z dz'\, \varphi(r,z') \quad . \tag{7}$$

Clearly the assumption of forward scattering (a) requires F, and therefore φ, to vanish as r approaches zero. By taking the Laplace transform of equation (7) with respect to the variable r, i.e. $L(\ldots) = \int_0^\infty dr\, e^{-rs}(\ldots)$, one obtains:

$$(s + z)\, f(s,z) = 1/s + \alpha \int_0^z dz' f(s,z'). \tag{8}$$

Where $f(s,z) = L\varphi(r,z)$.

Differentiating (8) with respect to s one obtains $\partial/\partial s\left[\ln f(s,z)\right] = (\alpha - 1)/(s + z)$, which has the solution $f(s,z) = A(s,\alpha)(s + z)^{\alpha - 1}$. The constant of integration $A(s,\alpha)$, is determined by substituting this solution into Equ. (8). In this manner one obtains:

$$f(s,z) = s^{-(\alpha + 1)}(s + z)^{\alpha - 1} \tag{9}$$

To obtain $\varphi(r,z)$ the inverse Laplace transform of f(s,z) is required*.

---

* See "Collected Papers of Geo. A. Campbell", pp 443 and 320

$$\mathcal{P}(r,s) = L^{-1}f(s,s) = r\ {}_1F_1\ (1 - \alpha\ ;\ 2;\ -sr)\ . \qquad (10)$$

Here ${}_1F_1\ (a;b;x) = \sum_{n=0}^{\infty} \frac{\Gamma(a+n)\cdot\Gamma(b)\cdot x^n}{\Gamma(a)\cdot\Gamma(b+n)\cdot n\ !}$ is the confluent hypergeometric series or the so-called modified Kummer function.

The yield of γ,n neutrons in a sphere of radius R is made up of two parts. The fraction arising from the first collisions of the primary photons is

$$F_\gamma(1 - e^{-x}). \qquad (11)$$

Here F_γ is the fraction of the primary photons that would be absorbed in the γ,n reaction upon first collision in an infinite sphere of D_2O. $\mu_\gamma\ (E_o)/\mu_o$, and x is the sphere radius in units of the primary photon mean free path; $x = \mu_o R$. The yield of second and higher collisions is given by $\int_{E_1}^{E} dE\mu_\gamma(E) \int_0^R drF(r,E)$ which becomes, upon introducing the expressions (8) and (10)

$$F_\gamma \cdot D \qquad (12)$$

Where $D = \left[\sigma(E_o \rightarrow E)/\sigma(E_o)\right] \int_{E_1}^{E_o} dE(\mu_\gamma(E)/\mu_\gamma(E_o)) \sum_{n=o}^{\infty} \frac{\Gamma(n-\frac{1}{4})(-B)^n}{\Gamma(-\frac{1}{4})n\ !} P_n(x)$

Here B is an energy dependent function which is, according to the approximation (3),

$$B = (\mu(E) - \mu_o)/\mu_o \approx (E_o/E - 1)/(1 + .069\ \alpha\ E_o). \qquad (13)$$

and $P_n(x)$ is the integrated Poisson collision distribution of constant mean free path forward collisions; n = o corresponds to second collisions, n = 1 to third, etc.

$$P_n(x) = \int_o^x dx e^{-x} x^{n+1}/(n+1)\,! = 1 - e^{-x} \sum_{i=o}^{n+i} x^i/i\,! \qquad (14)$$

The lower energy limit E_1 in (12) is the γ,n threshold, 4.8 mc^2.

The γ,n yield from all collisions in an infinite sphere of D_2O is the sum of (11) and (12) for $x = \infty$ namely, F_γ,E where

$$E = 1 + \left[\sigma(E_o \rightarrow E)/\sigma_o\right] \int_{E_1}^{E_o} dE \left[\mu_\gamma(E)/\mu_\gamma(E_o)\right] (1+E)^{\frac{1}{2}} \qquad (15)$$

Neglecting all except first collisions, the ratio between the finite and infinite sphere yield is

$$F_t = 1 - e^{-x} \qquad (16)$$

Taking into account second and higher collisions, one obtains the ratio between the infinite and finite sphere yield by multiplying the first collision yield ratio, $1/F_t$, by a factor β where

$$\beta = E/(1 + D/F_t) \qquad (17)$$

The quantities D and E defined by equations (12) and (15) were obtained by numerical integration over the γ-ray energies above the γ,n threshold. Dropping terms beyond n = 2 in the series appearing in Equ. (12) introduced an error in D of less than 0.2%.

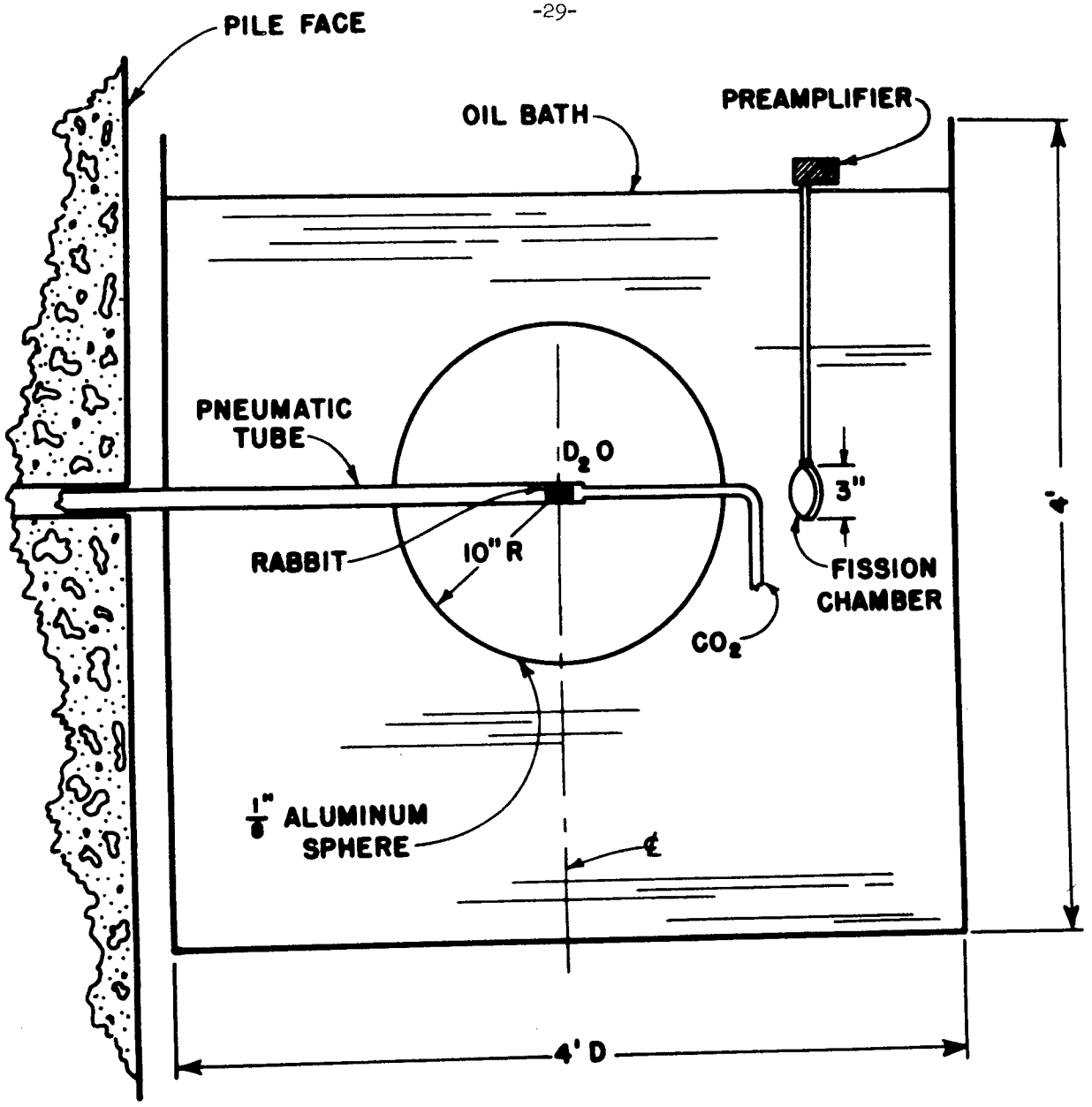

Dr. 3007
9-24-46

FIG. 1

SCHEMATIC DIAGRAM OF APPARATUS

Dr. 3008
9-24-46

SAMPLE OF FILM-RECORDED DATA

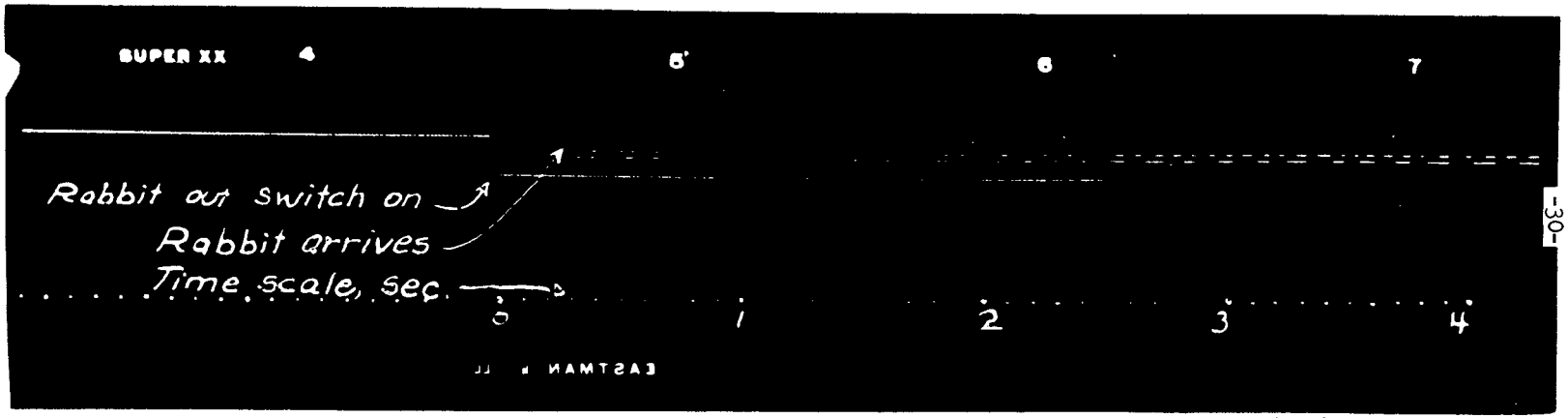

—Fig. 2—

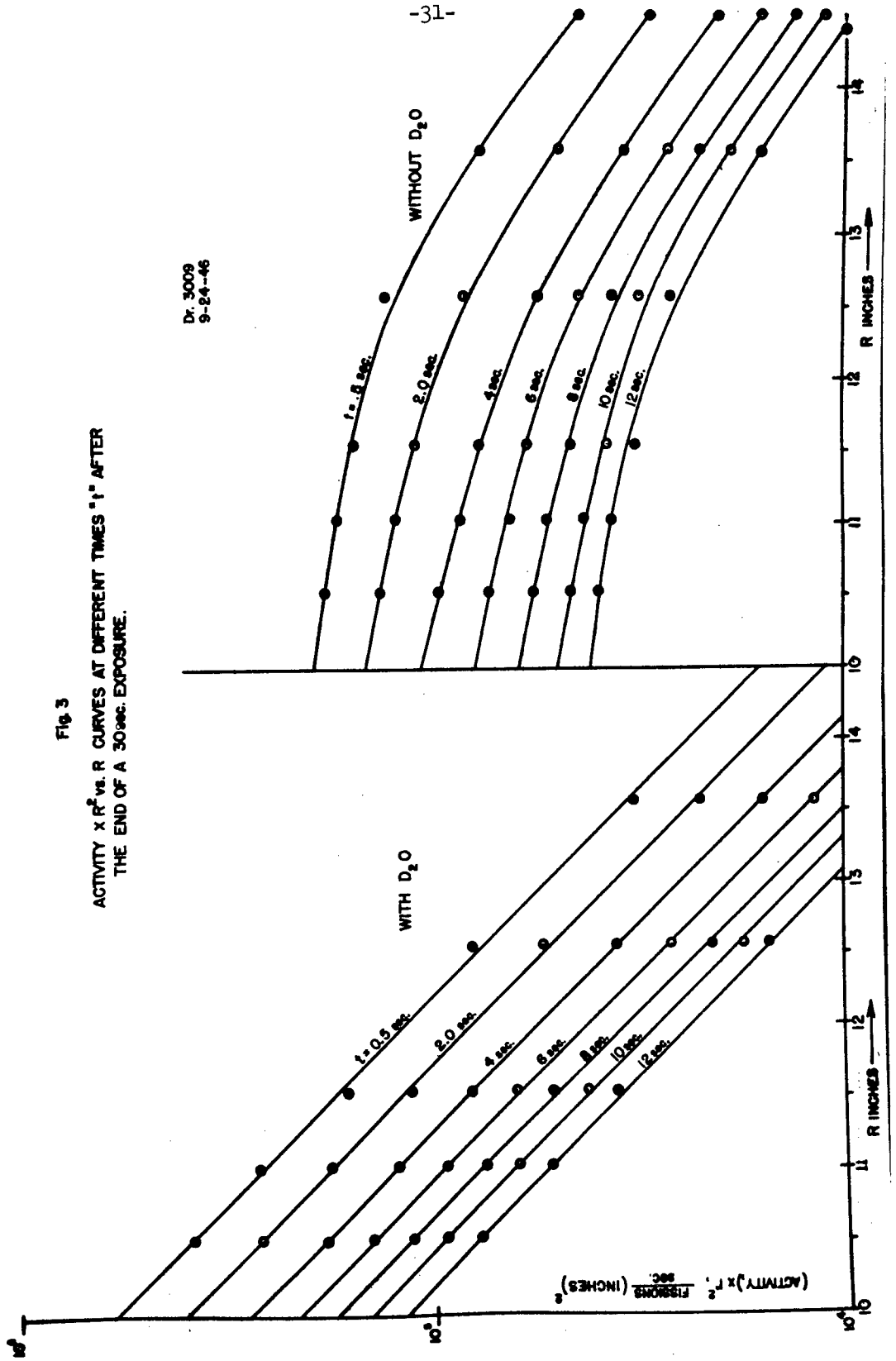

Fig. 3

ACTIVITY x R^2 vs. R CURVES AT DIFFERENT TIMES "t" AFTER THE END OF A 30sec. EXPOSURE.

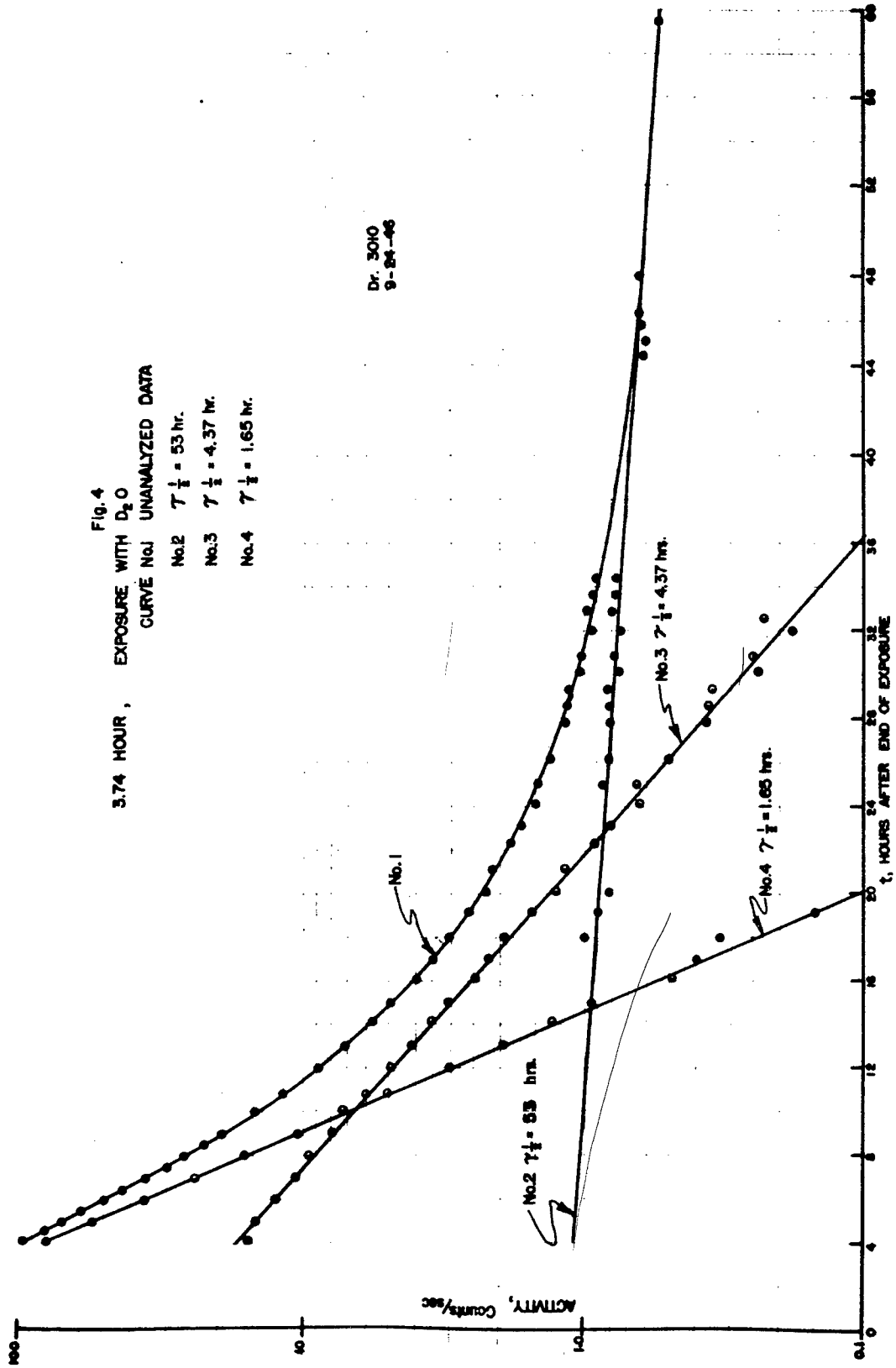
Fig. 4
3.74 HOUR, EXPOSURE WITH D_2O
CURVE No. UNANALYZED DATA
No.2 $T\frac{1}{2}$ = 53 hr.
No.3 $T\frac{1}{2}$ = 4.37 hr.
No.4 $T\frac{1}{2}$ = 1.65 hr.
Dr. 3OHO
9-24-46
No.1
No.2 $T\frac{1}{2}$ = 53 hrs.
No.3 $T\frac{1}{2}$ = 4.37 hrs.
No.4 $T\frac{1}{2}$ = 1.65 hrs.
ACTIVITY, Counts/sec
t, HOURS AFTER END OF EXPOSURE

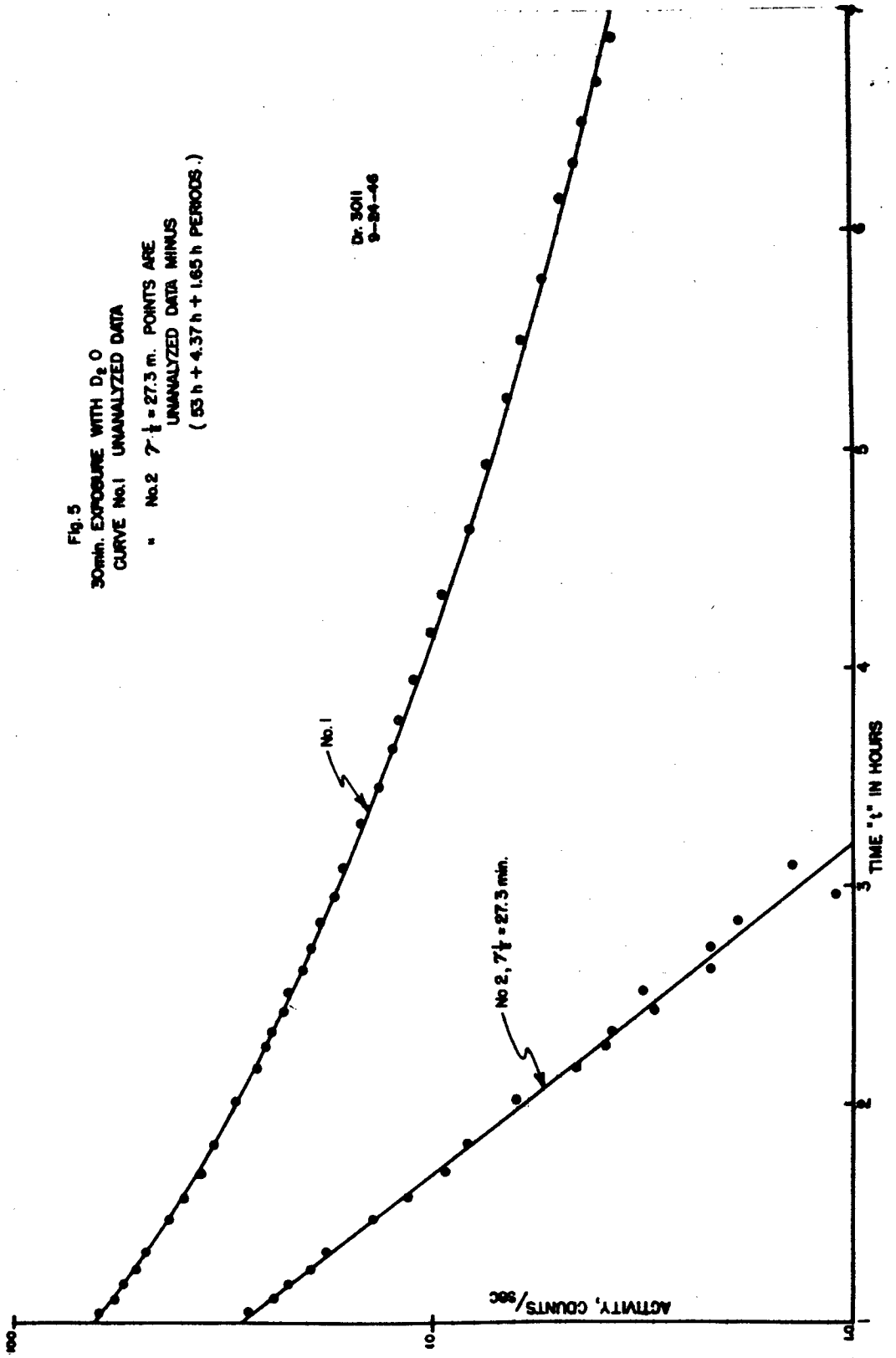
Fig. 5
30min. EXPOSURE WITH D_2O
CURVE No.1 UNANALYZED DATA
" No.2 $7\frac{1}{2}$ = 27.3 m. POINTS ARE
UNANALYZED DATA MINUS
(53 h + 4.37 h + 1.65 h PERIODS)
Dr. 3011
9-24-46
No.1
No 2, $7\frac{1}{2}$ = 27.3 min.
ACTIVITY, COUNTS/sec
TIME "t" IN HOURS
100
10
1
1
2
3
4
5
6

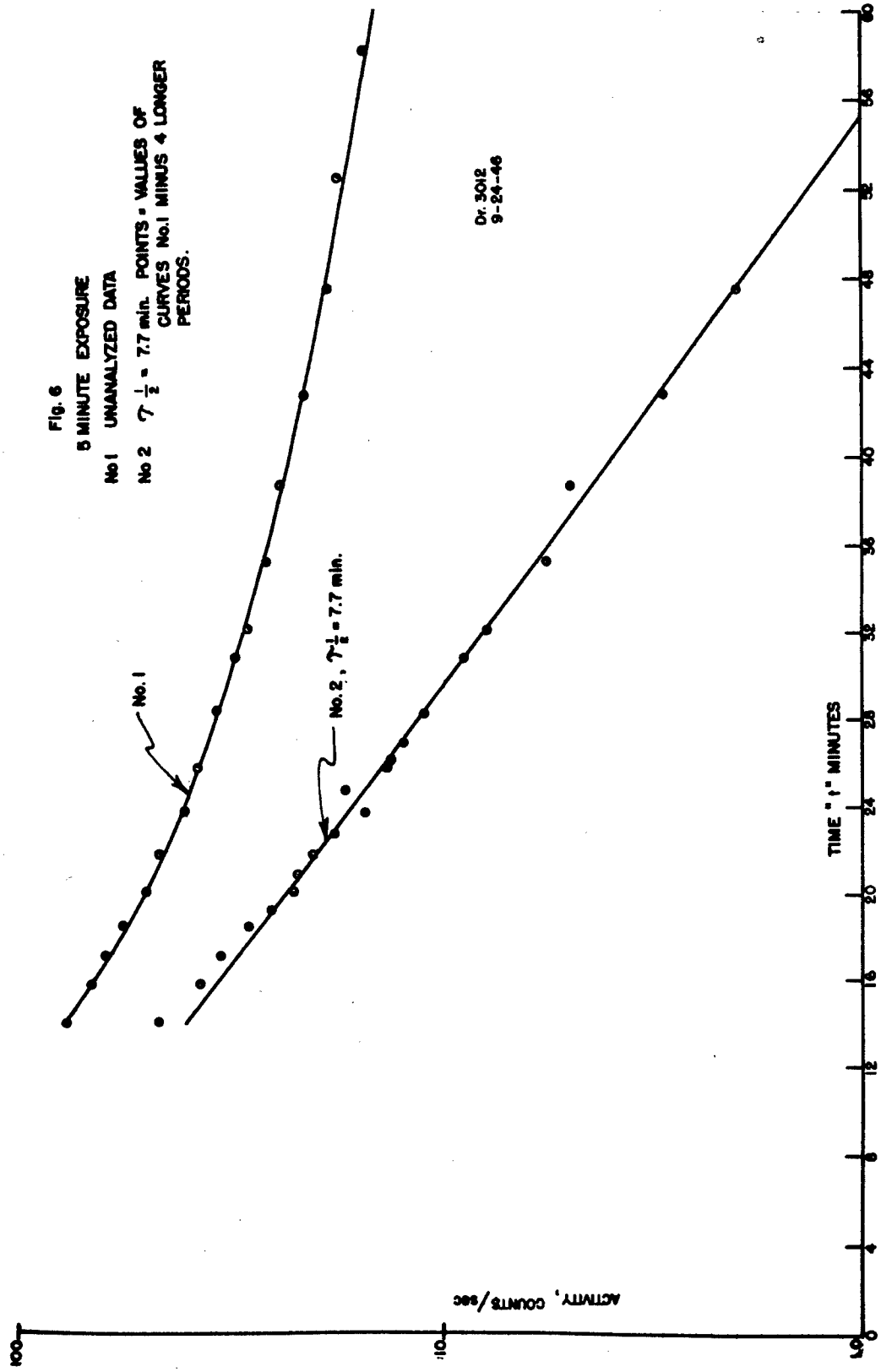
Fig. 6
5 MINUTE EXPOSURE
No 1 UNANALYZED DATA
No 2 $T\frac{1}{2}$ = 7.7 min. POINTS = VALUES OF CURVES No.1 MINUS 4 LONGER PERIODS.
Dr. 3012
9-24-46
No. 1
No. 2, $T\frac{1}{2}$ = 7.7 min.
ACTIVITY, COUNTS/sec
TIME "t" MINUTES
100
10
1.0
0
4
8
12
16
20
24
28
32
36
40
44
48
52
56
60

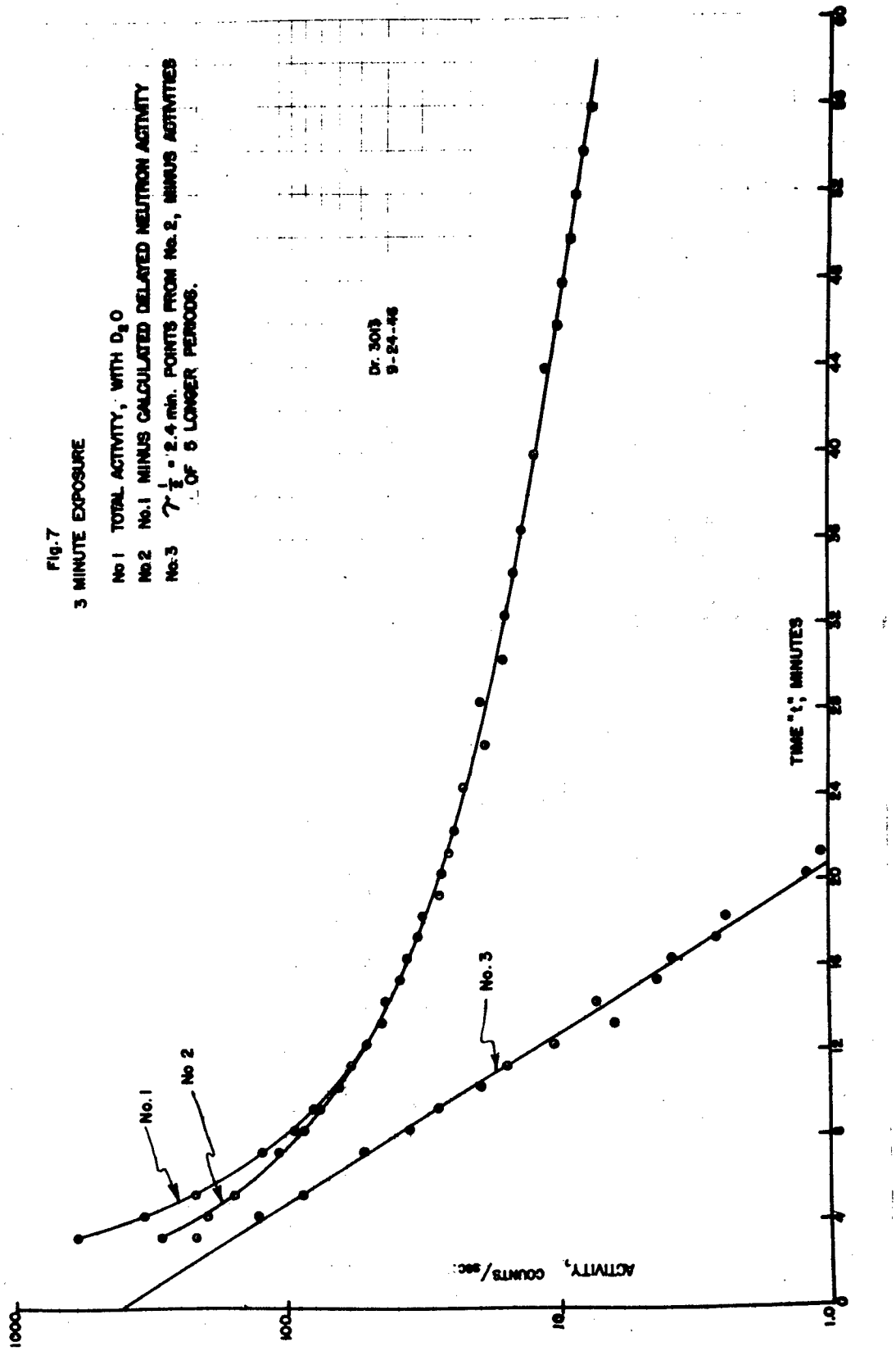
Fig.7
3 MINUTE EXPOSURE
No 1 TOTAL ACTIVITY, WITH D_2O
No.2 No.1 MINUS CALCULATED DELAYED NEUTRON ACTIVITY
No.3 $T_{\frac{1}{2}}$ = 2.4 min. POINTS FROM No. 2, MINUS ACTIVITIES OF 5 LONGER PERIODS.
Dr. 3013
9-24-46
No.1
No 2
No.3
ACTIVITY, COUNTS/sec.
TIME "t", MINUTES
1000
100
10
1.0
0
4
8
12
16
20
24
28
32
36
40
44
48
52
56
60

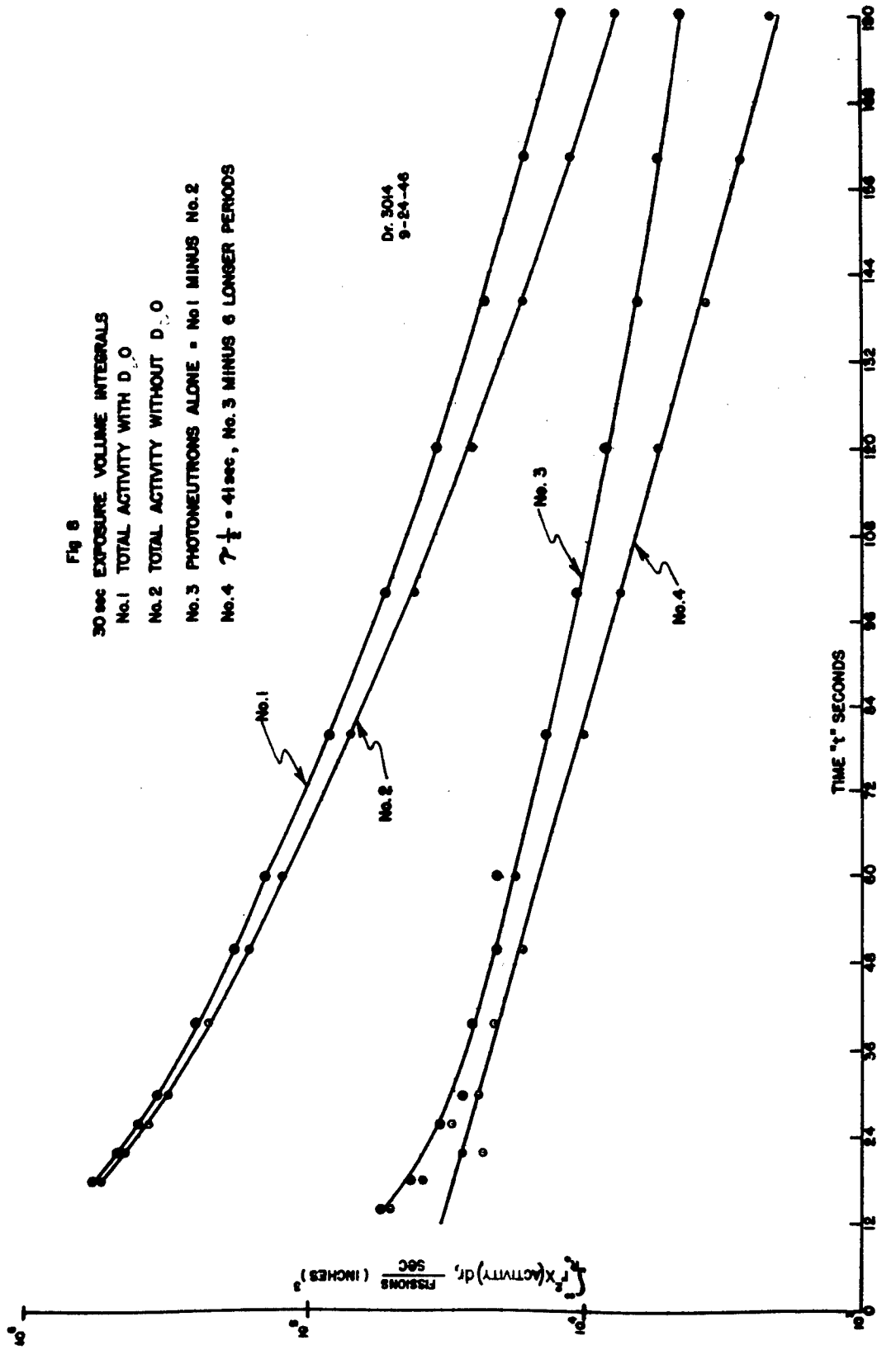
Fig 8
30 sec EXPOSURE VOLUME INTEGRALS
No.1 TOTAL ACTIVITY WITH D2O
No.2 TOTAL ACTIVITY WITHOUT D2O
No.3 PHOTONEUTRONS ALONE = No.1 MINUS No.2
No.4 T½ = 41 sec, No.3 MINUS 6 LONGER PERIODS
Dr. 3044
9-24-46
No.1
No.2
No.3
No.4
TIME "t" SECONDS
FISSIONS/SEC (INCHES)³

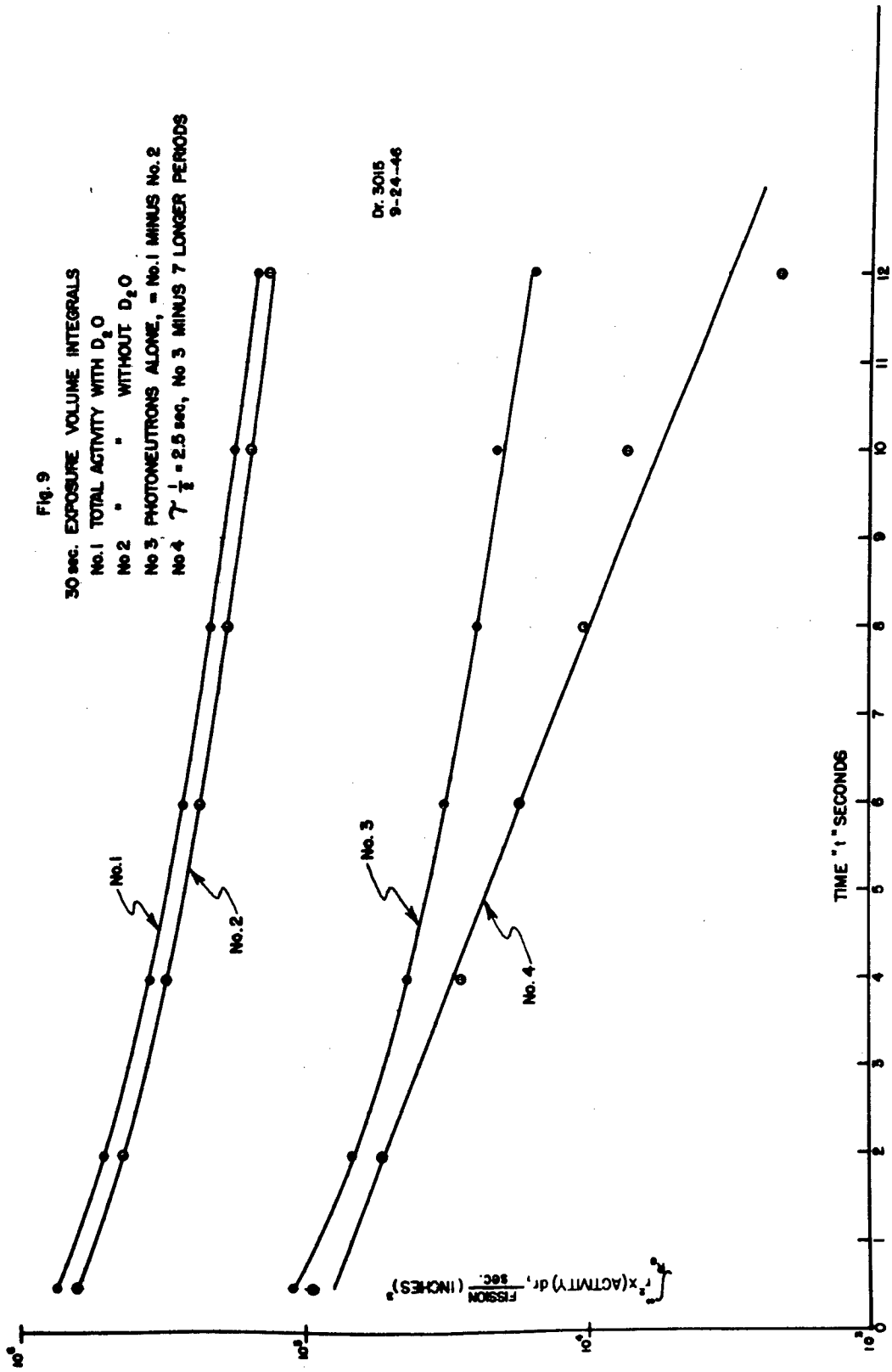

☆ U. S. GOVERNMENT PRINTING OFFICE: 1956 O—375238